

MIMO-OFDM for High Rate Underwater Acoustic Communications

Baosheng Li, *Student Member, IEEE*, Jie Huang, Shengli Zhou, *Member, IEEE*, Keenan Ball, Milica Stojanovic, *Member, IEEE*, Lee Freitag, *Member, IEEE*, and Peter Willett, *Fellow, IEEE*

Abstract—Multiple-input multiple-output (MIMO) techniques have been actively pursued in underwater acoustic communications recently to increase the data rate over the bandwidth-limited channels. In this paper, we present a MIMO system design, where spatial multiplexing is applied with OFDM signals. The proposed receiver works on a block-by-block basis, where null subcarriers are used for Doppler compensation, pilot subcarriers are used for channel estimation, and a MIMO detector consisting of a hybrid use of successive interference cancellation and soft MMSE equalization is coupled with LDPC channel decoding for iterative detection on each subcarrier. The proposed design has been tested using data recorded from three different experiments. A spectral efficiency of 3.5 bits/sec/Hz was approached in one experiment, while a data rate of 125.7 kb/s over a bandwidth of 62.5 kHz was achieved in another. These results suggest that MIMO-OFDM is an appealing solution for high data rate transmissions over underwater acoustic channels.

I. INTRODUCTION

To enhance the transmission rate over communication links, either the bandwidth, or the spectral efficiency in the unit of bits/sec/Hz, or both, need to be increased. Multi-input multi-output (MIMO) techniques can drastically increase the spectral efficiency via parallel transmissions over multiple transmitters [3], [4], hence are attractive to underwater acoustic communications which are inherently bandwidth-limited.

Recently, several different approaches have been investigated for MIMO underwater acoustic communications, including those for single carrier transmissions [5]–[11] and those for multicarrier transmissions in the form of orthogonal-frequency-division-multiplexing (OFDM) [1], [2], [12], [13]. Specifically, adaptive multichannel decision-feedback equalization (DFE) has been used in [5], [6] while a time-reversal preprocessing followed by a single channel equalizer has been

B. Li and S. Zhou are supported by the ONR YIP grant N00014-07-1-0805, the NSF grant ECCS-0725562, and the NSF grant CNS-0721834. J. Huang and P. Willett are supported by the ONR grant N00014-07-1-0429. K. Ball and L. Freitag are supported by the ONR grant N00014-07-1-0229. M. Stojanovic is supported by the ONR grants N00014-07-1-0202 and N00014-07-1-0738. Partial results have been presented in the MTS/IEEE OCEANS conference, Vancouver, Canada, Oct. 2007 [1] and the MTS/IEEE OCEANS conference, Quebec City, Canada, Sept. 2008 [2].

Associate Editor: H. Song.

B. Li, J. Huang, S. Zhou, and P. Willett are with the Dept. of Elec. and Computer Engr., University of Connecticut, Storrs, CT 06269; Emails: ({baosheng.jhuang.shengli.willett}@engr.uconn.edu).

K. Ball and L. Freitag are with the Woods Hole Oceanographic Institution, Woods Hole, MA 02543. Emails: (kball@whoi.edu, lfreitag@whoi.edu).

M. Stojanovic is with the Dept. of Elec. and Computer Engr., Northeastern University, MA. Email: (millitsa@mit.edu).

Publisher Item Identifier

used in [7], [8]. In [5], [6] and [7], [8], parameter adaptation is performed on a symbol by symbol basis. Adaptive block equalization techniques have been proposed in time domain [9] and in frequency domain [10], where parameter adaptation is carried over successive blocks. Using basis expansion models (BEM) to parameterize underwater acoustic channels, block-differential space time coding has been investigated in [11]. For multicarrier systems, a non-adaptive block-by-block design was presented in [1], [2], which is built upon the receiver developed for single-transmitter OFDM in [14], while a block-adaptive approach was developed in [12], which is built upon the single-transmitter OFDM system in [15], [16]. In [13], experimental results were presented for both coherent and differential designs in an OFDM system with two transmitters.

The objective of this paper is to present a MIMO-OFDM system design [1], [2] and report on the performance results with data recorded from various experiments. The proposed MIMO-OFDM design consists of the following key components: (1) null subcarriers are inserted at the transmitter to facilitate the compensation of Doppler shifts at the receiver; (2) pilot tones are used for MIMO channel estimation, and (3) an iterative receiver structure is adopted that couples MIMO detection with channel decoding. The MIMO detector applied on each OFDM subcarrier consists of a hybrid successive interference canceller and MMSE equalizer with *a priori* information [17], while the codes used are the nonbinary low-density parity-check (LDPC) codes from [18]. Note that an iterative receiver has been investigated in [19] for an underwater OFDM system with one transmitter, where carrier synchronization, channel estimation, and channel decoding are coupled. Our receiver does not include carrier synchronization and channel estimation in the loop. It rather focuses on the iterative processing between the MIMO detection and channel decoding.

The proposed design has been tested using data recorded from three different experiments: i) the AUV Fest, Panama City, FL, June 2007, ii) the RACE experiment in the Narragansett Bay, Rhode Island, March 2008, and iii) the VHF experiment conducted at the Buzzards Bay, MA, April 2008. For convenience, we will term these experiments as AUV07, RACE08, and VHF08 hereafter. With QPSK modulation, rate 1/2 coding, and a 12 kHz bandwidth, the achieved data rate in AUV07 was 12.18 kb/s. For the RACE08 experiment, we report MIMO-OFDM performance results of QPSK/8-QAM/16-QAM/64-QAM with two transmitters,

QPSK/8-QAM/16-QAM with three transmitters, and QPSK/8-QAM with four transmitters where a bandwidth of 4.9 kHz is used. A spectral efficiency of 3.5 bits/sec/Hz was approached with various configurations. In the VHF08 experiment, a data rate of 125.7 kb/s was achieved with two transmitters, 16-QAM modulation, rate 1/2 coding, and a bandwidth of 62.5 kHz. These results suggest that MIMO-OFDM is an appealing solution for very high data rate transmissions over underwater acoustic channels.

The rest of the paper is organized as follows. We describe the transmitter design in Section II and present the receiver algorithms in Section III. Performance results for different experiments are summarized in Sections IV, V, and VI. Conclusions are drawn in Section VII.

Notation: Bold upper and lower letters denote matrices and column vectors, respectively; $(\cdot)^T$, $(\cdot)^*$, and $(\cdot)^H$ denote transpose, conjugate, and Hermitian transpose, respectively; \mathbf{I}_N is the $N \times N$ identity matrix.

II. TRANSMITTER DESIGN

We consider MIMO-OFDM transmission with spatial multiplexing on N_t transmitters. The basic signalling format is zero-padded (ZP) OFDM [14]. Specifically, let B denote the bandwidth and K the number of subcarriers. The subcarrier spacing is $\Delta f = B/K$ and the OFDM block duration is $T = 1/\Delta f = K/B$. Each OFDM block is followed by a guard time of duration T_g to avoid interblock interference. Out of the total K subcarriers, K_n subcarriers are null subcarriers where no information will be transmitted, K_p subcarriers are pilot subcarriers carrying known symbols, and the rest $K_d = K - K_n - K_p$ subcarriers are data subcarriers.

The signals are generated as follows. Let r_c denote the code rate of channel code and M the size of the constellation, which could be 4, 8, 16, or 64 in our experiments. For each OFDM block, we generate N_t independent bit streams each of length $r_c K_d \log_2 M$ and encode them separately using the nonbinary low-density-parity-check (LDPC) codes [18]. Each coded bit stream of length $K_d \log_2 M$ is mapped into a symbol sequence of length K_d . A total of N_t OFDM blocks are formed with each block carrying K_d symbols from one symbol sequence. After proper pilot insertions, the N_t OFDM blocks are transmitted from N_t transmitters simultaneously. The next N_t blocks then follow.

Accounting for all the overheads due to the guard interval, channel coding, pilot, and null subcarriers, the overall spectral efficiency in terms of bits per second per Hz (bits/s/Hz) is:

$$\alpha = N_t \cdot \frac{T}{T + T_g} \cdot \frac{K_d}{K} \cdot r_c \cdot \log_2 M. \quad (1)$$

With a bandwidth B , the data rate in the unit of bits/s is

$$R = \alpha B. \quad (2)$$

In this paper, we will include experimental results with $N_t = 2, 3, 4$ transmitters. The total number of pilot subcarriers for all transmitters is K_p . Specifically, we will use a total of $K_p = K/4$ pilot subcarriers in our experimental results. To simplify channel estimation, each transmitter will be allocated a set of non-overlapping pilot subcarriers to transmit nonzero

pilot symbols, while zeros are transmitted on those subcarriers that belong to other transmitters. When $N_t = 2$ and $N_t = 4$, each transmitter μ will be assigned $K_p/N_t = K/(4N_t)$ subcarriers that are equally spaced. For example, one assignment on the pilot indexes to the μ th transmitter, where $\mu = 1, \dots, N_t$, could be $\{4N_t(i-1) + 4(\mu-1) + 2\}_{i=1}^{K/(4N_t)}$. When $N_t = 3$, the pilot positions are identical to the $N_t = 4$ case, simply turning off one transmitter from the 4-transmitter system. The null subcarrier positions are identical for all transmitters. Half of null tones are placed at the edges of the frequency band, while the other half are randomly drawn from the available subcarrier positions. The positions of null subcarriers are fixed for all blocks after being picked during the design phase.

III. RECEIVER ALGORITHMS

The receiver algorithms should be well designed for the underwater acoustic communications. For stationary MIMO-OFDM tests, no resampling operation as described in [14] was needed. The key processing steps at the receiver are depicted in Fig. 1, and will be described next.

A. Doppler estimation

The channel Doppler effect can be viewed as caused by carrier frequency offsets (CFO) among the transmitters and the receivers [14]. On each receiver, we assume a common CFO relative to all transmitters, as in [20, Chapter 11.5]. Hence, the CFO estimation algorithm presented in [14, Eqns. (14) and (15)] is directly applicable, where the energy on the null subcarriers is used as the objective function to search for the best CFO estimate.

After Doppler shift estimation and compensation, the average energy on the null subcarriers is used to compute the variance of the additive noise and residual inter-carrier-interference (ICI). This quantity is needed for the soft MMSE equalization in Section III-C.

B. Channel estimation

After CFO compensation, pilot tones are used for channel estimation. Note that at each receive antenna ν , a total of N_t channels $\{\mathbf{h}_{\nu,\mu} := [h_{\nu,\mu}(0), \dots, h_{\nu,\mu}(L-1)]^T\}_{\mu=1}^{N_t}$ need to be estimated, where L is the channel length and $h_{\nu,\mu}(l)$ is the l th channel tap of the baseband equivalent model.

Since each transmitter is assigned with an exclusive set of pilot subcarriers, channel estimation is carried out for each transmitter-receiver pair separately. With equally-spaced pilot tones, the least-square (LS) channel estimator does not involve matrix inversion and can be implemented by an K_p/N_t -point inverse fast Fourier transform (FFT), as described in [14, eqns. (18) and (19)]. Once the channel estimates $\hat{\mathbf{h}}_{\nu,\mu}$, $\mu = 1, \dots, N_t$, $\nu = 1, \dots, N_r$, are available, the channel frequency response on each data subcarrier k is evaluated as

$$\hat{H}_{\nu,\mu}[k] = \sum_{l=0}^{L-1} \hat{h}_{\nu,\mu}(l) e^{-j2\pi kl/K}. \quad (3)$$

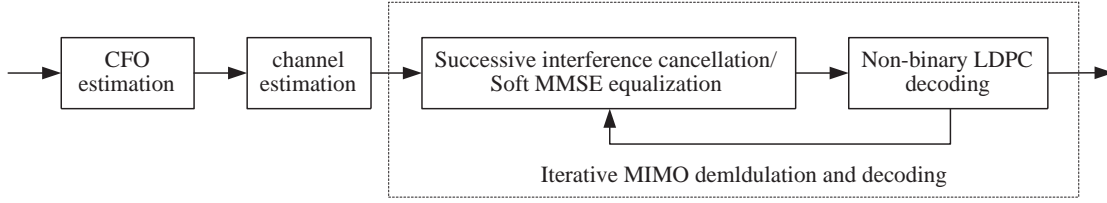


Fig. 1. The receiver block diagram

Since K_p/N_t pilot tones are used for each channel estimator, our transceiver design can handle channels with $L \leq K_p/N_t$ taps, which corresponds to a delay spread of $K_p/N_t/B$ seconds. To handle longer channels, sparse channel estimation based on irregularly spaced pilot tones can be pursued (see e.g., [21]), which is outside the scope of this paper.

C. Iterative MIMO demodulation and decoding

On each data subcarrier k , the data from N_r receiving elements is grouped into a vector $\mathbf{y}[k] = [y_1[k], \dots, y_{N_r}[k]]^T$. The vector $\mathbf{s}[k] := [[s_1[k], \dots, s_{N_t}[k]]^T$ contains the transmitted symbols on the k th subcarrier from N_t transmitters, and $\hat{\mathbf{H}}[k]$ denotes the $N_r \times N_t$ channel matrix with $\hat{H}_{\nu,\mu}[k]$ as its (ν, μ) th entry. We thus have:

$$\mathbf{y}[k] = \hat{\mathbf{H}}[k]\mathbf{s}[k] + \mathbf{w}[k], \quad (4)$$

where $\mathbf{w}[k]$ contains the additive noise and residual ICI. We assume that the noises on different receivers are uncorrelated and Gaussian distributed, where the noise variance is estimated as the average energy on the null subcarriers. For convenience of algorithm presentation, the data are properly scaled so that the noise variances are identical for all receivers. In other words, $\mathbf{w}[k]$ is assumed to be additive white Gaussian noise.

A maximum a posteriori (MAP) MIMO detector and a linear zero-forcing (ZF) detector were presented in [1] for the setting of two transmitters and QPSK modulation. In this paper, we combine successive interference cancellation (SIC), the soft MMSE equalization method developed in [17], and the nonbinary LDPC decoding in [18] to develop an iterative procedure on MIMO demodulation and decoding. The steps are as follows.

- **Step 1: Initialization.**

First, we define N_t flags to indicate the decoding success on parallel data streams. Initially all flags are set to zero implying no success.

Second, for each symbol in (4) to be demodulated, the mean is set to zero and the variance to the symbol energy E_s , i.e., initially each symbol has equal probability of residing on all the constellation points.

Third, to reduce the complexity of MMSE equalization, we project the $N_r \times 1$ received vector onto the N_t dimensional signal space as N_r might be much larger than N_t . (This step is *optional*, but can reduce the matrix size for the subsequent iterative MIMO equalization without compromising the performance.) Specifically, let $\mathbf{U}[k]$ contain N_t basis vectors of the range space of $\hat{\mathbf{H}}[k]$, which can be found by singular value decomposition. We

obtain

$$\tilde{\mathbf{z}}[k] = \mathbf{U}^H[k]\mathbf{y}[k] = \tilde{\mathbf{A}}[k]\mathbf{s}[k] + \boldsymbol{\xi}[k], \quad (5)$$

where $\tilde{\mathbf{A}}[k] = \mathbf{U}^H[k]\hat{\mathbf{H}}[k]$ is now a square matrix and $\boldsymbol{\xi}[k] = \mathbf{U}^H[k]\mathbf{w}[k]$ has the same covariance as $\mathbf{w}[k]$.

- **Step 2: Interference cancellation.**

The data streams which are declared with decoding success do not need to be decoded again. Hence, their contributions can be subtracted from the received signals. Assume that N out of N_t data streams remain to be decoded. Partition $\tilde{\mathbf{A}}[k]$ as $[\mathbf{A}_d[k], \mathbf{A}_u[k]]$, where the first part corresponds to the correctly decoded data streams and the second part corresponds to the remaining streams. Similar partition is performed for $\mathbf{s}_d[k]$ and $\mathbf{s}_u[k]$. We then obtain

$$\mathbf{z}[k] = \tilde{\mathbf{z}}[k] - \mathbf{A}_d[k]\mathbf{s}_d[k] = \mathbf{A}_u[k]\mathbf{s}_u[k] + \boldsymbol{\xi}[k]. \quad (6)$$

- **Step 3: MMSE equalization with a priori information.**

On each subcarrier k , the MMSE equalization algorithm with *a priori* information from [17] is applied. The inputs to the MMSE equalizer are $\mathbf{z}[k]$, $\mathbf{A}_u[k]$, and the means and variances of all symbols comprising $\mathbf{s}_u[k]$. The outputs of the MMSE equalizer are the probabilities of each information symbol being equal to one valid constellation point. The details are provided in the Appendix.

- **Step 4: Nonbinary LDPC decoding.**

With the outputs from the MMSE equalizer, non-binary LDPC decoding [18] is run for each data stream to be decoded. The decoder yields the decoded information symbols and the updated probabilities, which are used to refine the mean and variance of each symbol as

$$\bar{s} = \sum_{\alpha_i \in \mathcal{S}} \alpha_i \cdot P(s = \alpha_i), \quad (7)$$

$$v = \left(\sum_{\alpha_i \in \mathcal{S}} |\alpha_i|^2 \cdot P(s = \alpha_i) \right) - |\bar{s}|^2, \quad (8)$$

where $\mathcal{S} = \{\alpha_1, \alpha_2, \dots, \alpha_M\}$ denotes the M -ary modulation alphabet.

During the decoding process, the decoder will declare success if the parity check conditions are satisfied.

- **Step 5: Iteration among steps 2, 3, and 4.**

The iteration will stop after one more round of decoding on the last data stream when the other $N_t - 1$ streams have been successfully decoded, or after a pre-specified number of runs.

IV. PERFORMANCE RESULTS: AUV07

The experimental data for this test was collected during the AUV Fest held in Panama City, FL, June 2007. The water depth was 20 meters. Two transmitters were deployed about 9 meters below a surface buoy. The receiving array was about 9 meters below a boat. The vertical array was 2 meters in aperture with 16 hydrophones, out of which we used four. Here we report performance results for transmission distances of 500 and 1500 meters. The key system parameters are listed in Table I.

TABLE I
SYSTEM PARAMETERS FOR AUV07

Sampling rate	$f_s = 96$ kHz
Center frequency	$f_c = 32$ kHz
Signal bandwidth	$B = 12$ kHz
OFDM block duration	$T = 85.33$ ms
Guard interval	$T_g = 25$ ms
Subcarrier spacing	$\Delta f = 11.72$ Hz
Number of subcarriers	$K = 1024$
Number of data carriers	$K_d = 672$
Number of pilot carriers	$K_p = K/4 = 256$
Number of null subcarriers	$K_n = 96$
Spectral efficiency (two transmitters, QPSK modulation, rate 1/2 coding)	$\alpha = 1.015$ bits/s/Hz
Data rate	$R = 12.18$ kb/s

A. Channel profiles via preamble correlation

A linearly-frequency-modulated (LFM) signal is used as a preamble for synchronization. The correlation results are shown in Fig. 2 for the 500 m case, and in Fig. 3 for the 1500 m case. It can be seen that the channel at 500 m has a larger delay spread than the channel at 1500 m, as expected.

B. CFO and channel estimation

The CFO estimates are shown in Fig. 4 for one data packet on one receiver. The CFO is within [-2, 2] Hz range, which is caused by transmitter and receiver drifting with waves.

The estimated channel for one OFDM block is shown in Fig. 5, which is in good agreement with the channel profiles shown in Figs. 2 and 3. It can be seen that the channel for the 500 m case has larger energy.

With $K_p/2 = 128$ subcarriers for each channel estimation, we can estimate 128 channel taps in discrete time, which amounts to a delay spread of 10.7 ms. Any arrivals after 10.7 ms will thus be treated as additive noise. Since the channel at 500 m has significant arrivals after 10.7 ms, the noise floor is much higher (around 8 dB) than that at 1500 m, as shown in Fig. 6. As a result, although the signal energy at 500 m is greater than that at 1500 m, the pre-demodulation signal to noise ratios (SNRs) become similar for both cases. The pre-demodulation SNR is computed as the ratio of the average signal energy on the pilot subcarriers to the average energy on the null subcarriers.

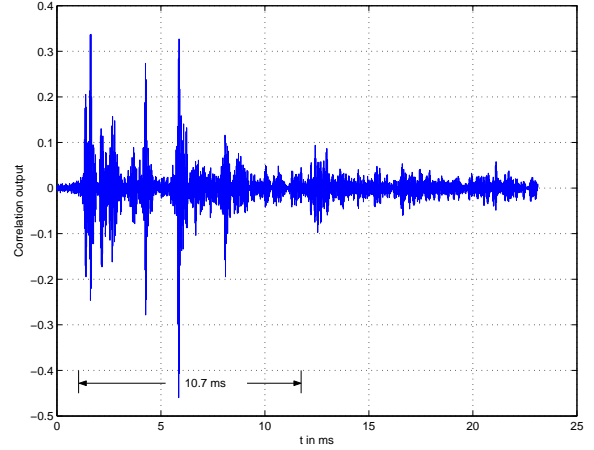


Fig. 2. Channel profile based on preamble correlation, 500 m, AUV07.

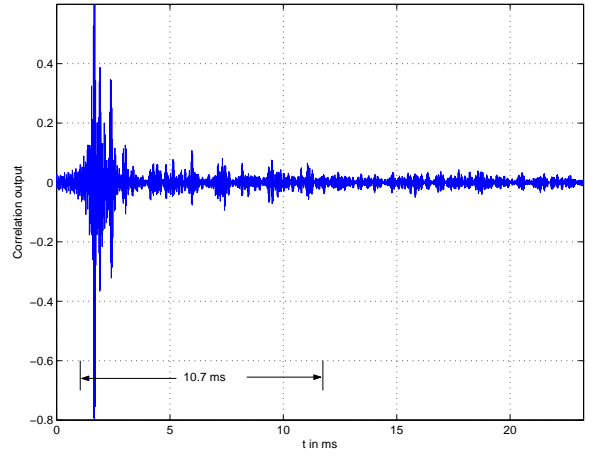


Fig. 3. Channel profile based on preamble correlation, 1500 m, AUV07.

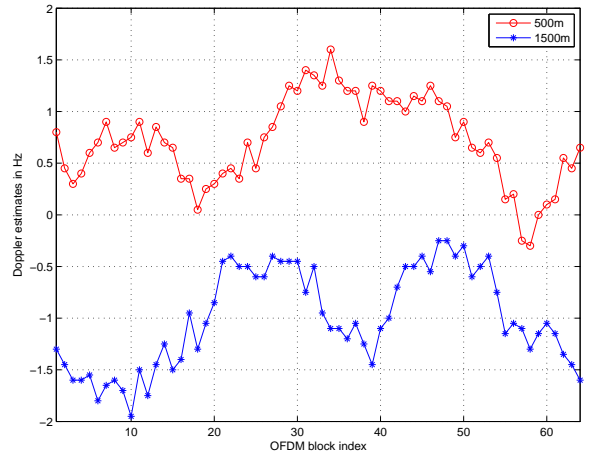


Fig. 4. Doppler estimates for one packet of 64 OFDM blocks at receiver 1; this Doppler shift is due to unintentional drifting.

C. BER results

We now report on the BER results, where QPSK modulation and rate 1/2 nonbinary LDPC coding are utilized and the data rate is 12.18 kb/s. A total of 64 OFDM blocks have been transmitted, and hence, each parallel data stream contains

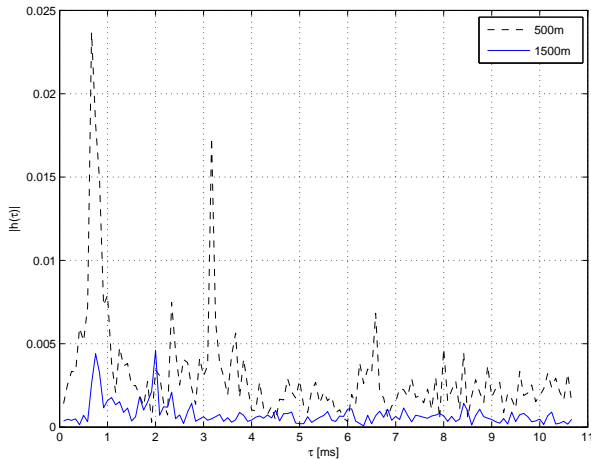


Fig. 5. Estimated channel for one OFDM block, receiver 1, AUV07.

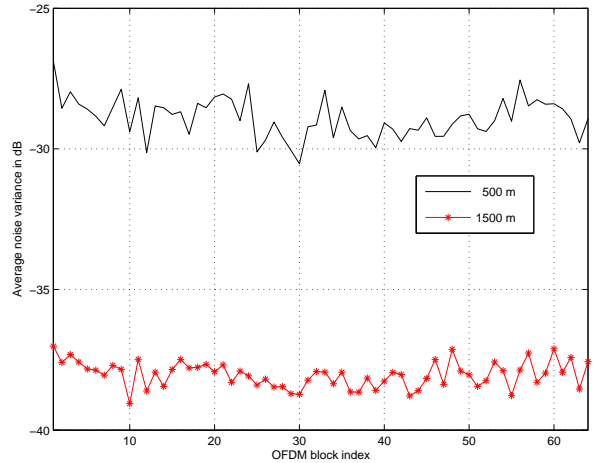


Fig. 6. Average noise variance on null subcarriers for one packet.

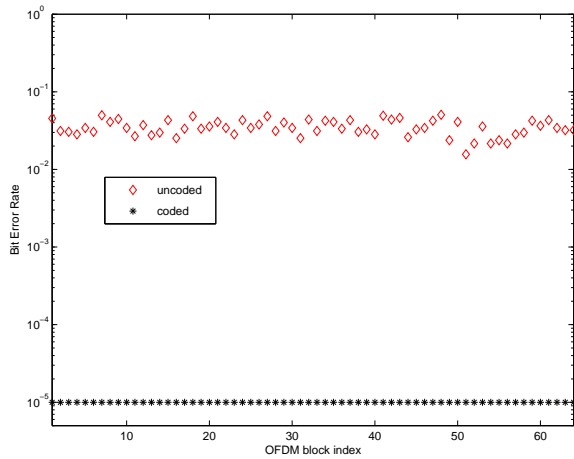


Fig. 7. The 500 m case in AUV07, data stream 1, MMSE equalization followed by LDPC coding; no block has decoding errors.

$672 \times 64 = 43008$ information bits. Figs. 7 and 8 show the uncoded and coded BERs for data streams 1 and 2 in the 500m case, respectively, where MMSE equalization is followed by LDPC decoding but *with no iteration*. Only two out of 64 blocks have decoding errors for data stream 2. For the 1500 m case, there is no error after LDPC decoding with the non-iterative receiver.

We then apply the iterative MMSE demodulation and channel decoding on the data of the 500 m case. There is no decoding error after one round of iteration.

V. PERFORMANCE RESULTS: RACE08

The Rescheduled Acoustic Communications Experiment (RACE) was held in the Narragansett Bay, Rhode Island, March 2008. The water depths in the area range from 9 to about 14 meters. The primary source of an ITC1007 transducer for acoustic transmissions was located approximately 4 meters above the bottom. A vertical source array consisting of three AT-12ET transducers with a spacing of 60 cm between each transducer was deployed below the primary source. The top of the source array was approximately 1 meter below the primary source. The system parameters are listed in Table II.

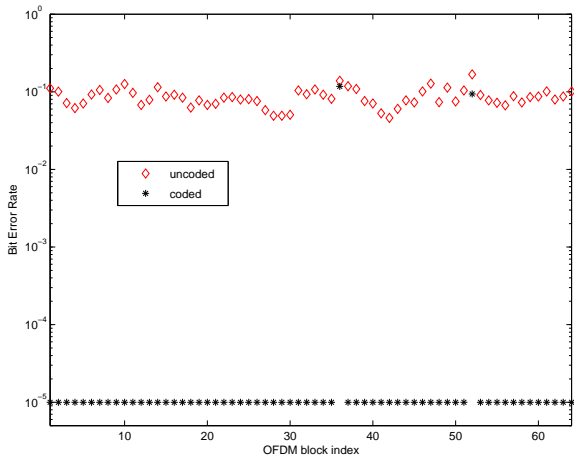


Fig. 8. The 500 m case in AUV07, data stream 2, MMSE equalization followed by LDPC coding; 2 out of 64 blocks have decoding errors.

TABLE II
THE SYSTEM PARAMETERS FOR THE RACE08 EXPERIMENT

Sampling rate	$f_s = 39.0625$ kHz
Center frequency	$f_c = 11.5$ kHz
Signal bandwidth	$B = 4.8828$ kHz
OFDM block duration	$T = 209.7152$ ms
Guard interval	$T_g = 25$ ms
Subcarrier spacing	$\Delta f = 4.8$ Hz
Number of subcarriers	$K = 1024$
Number of data carriers	$K_d = 672$
Number of pilot carriers	$K_p = K/4 = 256$
Number of null subcarriers	$K_n = 96$

The four transducers are labeled from top to bottom as T0, T1, T2 and T3. For MIMO-OFDM transmissions, T0 and T1 were used for two transmitters, T0-T2 for three transmitters, and T0-T3 for four transmitters. T0 and the T1-T3 array were driven by different power supplies and hence they have different front-end circuits. In addition, driven by the same voltage inputs, the transducer T0 produces less transmission power than T1-T3, about 5dB lower comparing the peaks. Finally, the spacing between T0 and T1 is greater than the

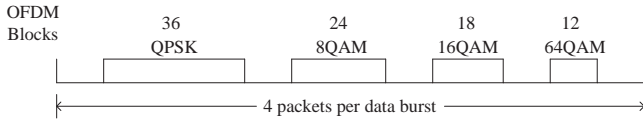


Fig. 9. The structure of the transmission file for RACE08.

spacings between T1, T2, T3. Such a disparity between T0 and T1-T3 renders the data stream from T0 at a disadvantage relative to the other data streams; this will be reflected by the performance results.

For each MIMO-OFDM configuration, one data burst consisted of four packets with different modulation formats, as shown in Fig. 9. In particular, the packet of QPSK modulation contains 36 OFDM blocks, the packet of 8-QAM contains 24 OFDM blocks, the packet of 16QAM contains 18 OFDM blocks, while the packet of 64-QAM contains 12 OFDM blocks. (The 8-QAM constellation used in this paper is from [22, Fig. 4.3-4]). Rate 1/2 nonbinary LDPC coding as described in [18] is applied. Hence, each data burst contains the same number ($672 \times 36 = 24192$) of information bits for each parallel data stream at each setting.

Three receiving arrays were deployed during the experiment, mounted on fixed tripods with the bottom of the arrays 2 meters above the sea floor. We here report on the results for the array at 400 meters to the east from the source, which is a 24-element vertical array with 5 cm between elements. (Note that half of the wavelength at the carrier frequency is about 6.5 cm. The responses on the array elements might be slightly correlated.) We will use the data from the top 12 elements for processing, where the iterative MMSE demodulation and decoding structure is employed.

During the experiment, each signal was transmitted twice every four hours, leading to 12 transmissions each day. We here report on the performance results based on data collected from 28 transmissions within the Julian dates 081-083 (March 21-23, 2008). Hence, each data stream at each setting has a total of $28 \times 24192 = 677,376$ information bits transmitted.

Fig. 10 depicts the channel estimates in one OFDM block with three transmitters, while Fig. 11 shows the channel estimates in one OFDM block with four transmitters (from a recorded block at the time 0200 GMT on the Julian date 081). The channel delay spreads are about 5 ms. Note that the channel corresponding to the first data stream (transducer T0) has lower energy than others. This is a general trend for all the received blocks, and is attributed to the implementation differences discussed earlier.

A. Performance results with two transmitters

Figs. 12–14 depict the coded block-error-rate (BLER) for each received data set across the Julian dates 081-083. The 8-QAM case is omitted as it has zero BLERs across all dates. Decoding errors occur only in one out of 28 data sets in the QPSK case, where two out of 36 OFDM blocks were badly distorted thus preventing correct decoding of stream 1. Table III summarizes the coded bit-error-rates (BERs) and BLERs averaged over all data sets; i.e., a total of 677,376 information bits was used for each BER computed in the table.

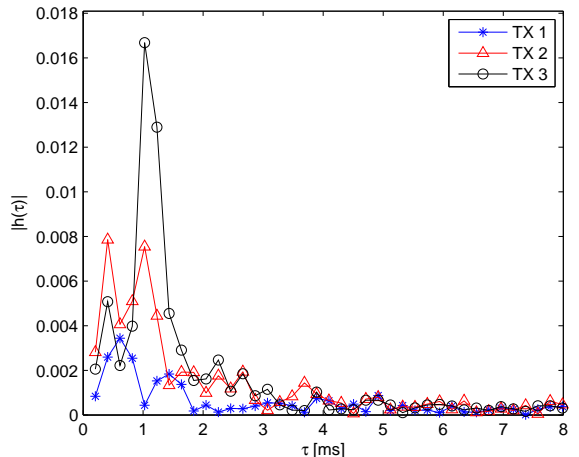


Fig. 10. Channel estimates from one OFDM block with three transmitters, RACE08.

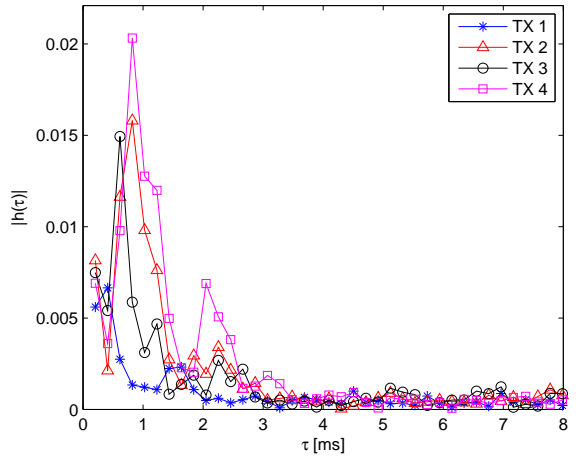


Fig. 11. Channel estimates from one OFDM block with four transmitters, RACE08.

B. Performance results with three transmitters

Figs. 15, 16, and 17 depict the coded BLER for each received data set across the Julian dates 081-083. Table IV summarizes the BERs and BLERs averaged over all data sets.

C. Performance results with four transmitters

Figs. 18 and 19 depict the coded BLER for each received data set across the Julian dates 081-083. Table V summarizes the BERs and BLERs averaged over all data sets.

Usually no more than five iterations were needed between MIMO demodulation and decoding. From Tables III–V, we observe that the data stream 1 has worse performance than the other data streams. This is partly due to the fact that the transducer on T0 has less power efficiency than others. We also conjecture that there might exist a possible Doppler shift mismatch between T0 and the array T1-T3 due to different spacings and front-end circuits. The BLER performance for all other data streams except stream 1 are acceptable and actually very good in many cases. A closer look at Figs. 15–19 reveals that no errors occurred in the majority of the data sets within

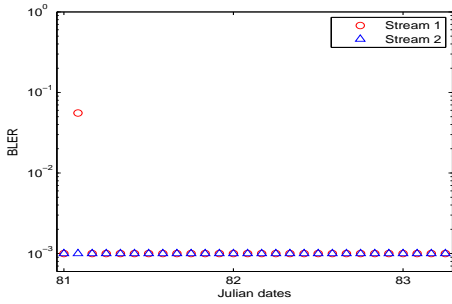


Fig. 12. Block error rates for 2IMO-OFDM, QPSK

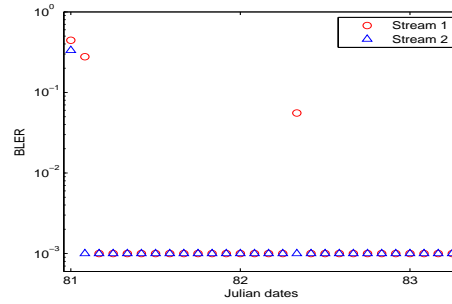


Fig. 13. Block error rates for 2IMO-OFDM, 16-QAM

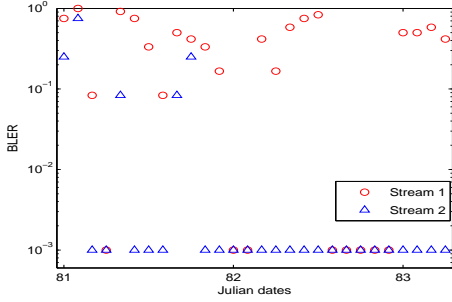


Fig. 14. Block error rates for 2IMO-OFDM, 64-QAM

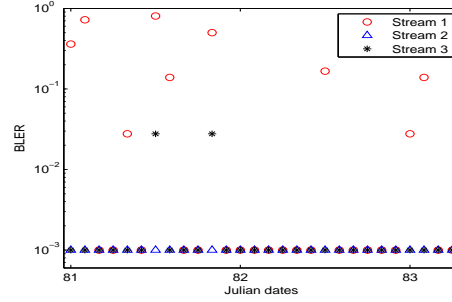


Fig. 15. Block error rates for 3IMO-OFDM, QPSK

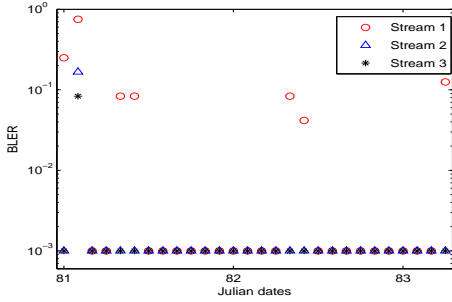


Fig. 16. Block error rates for 3IMO-OFDM, 8-QAM

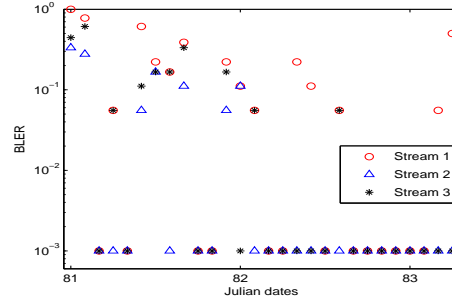


Fig. 17. Block error rates for 3IMO-OFDM, 16-QAM

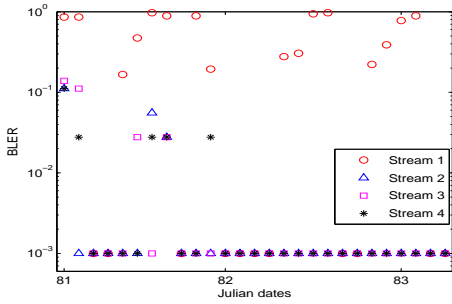


Fig. 18. Block error rates for 4IMO-OFDM, QPSK

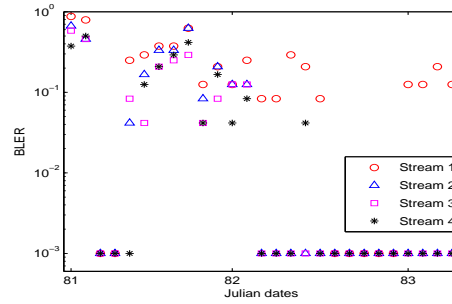


Fig. 19. Block error rates for 4IMO-OFDM, 8-QAM

the three-day span. The particular case of two transmitters and 8-QAM modulation having a spectral efficiency of 1.76 bits/s/Hz does not have any decoding error across all the 28 data sets across three days.

In short, the spectral efficiency can be increased considerably by using high order modulation in MIMO-OFDM transmissions, as demonstrated by the values corresponding to different configurations in Tables III–V. In particular, a

spectral efficiency of 3.52 bits/sec/Hz is approached by two parallel 64-QAM data streams, or three parallel 16-QAM data streams, or four parallel 8-QAM data streams¹.

¹Note that some of the high spectral efficiencies are obtained at relative high block error rates. In practice, a high-rate outer channel code could handle those block errors at a small rate loss. We thank one reviewer for pointing this out.

TABLE III
PERFORMANCE RESULTS WITH TWO TRANSMITTERS AND TWELVE RECEIVERS, RACE08

	Spectral efficiency	Data streams	Average BER	Average BLER
2IMO, QPSK	1.17 bits/s/Hz	Stream 1	$4 \cdot 10^{-4}$	$2 \cdot 10^{-3}$
		Stream 2	0	0
2IMO, 8-QAM	1.76 bits/s/Hz	Stream 1	0	0
		Stream 2	0	0
2IMO, 16-QAM	2.35 bits/s/Hz	Stream 1	$6 \cdot 10^{-3}$	$3 \cdot 10^{-2}$
		Stream 2	$3 \cdot 10^{-3}$	$1 \cdot 10^{-2}$
2IMO, 64-QAM	3.52 bits/s/Hz	Stream 1	$7 \cdot 10^{-2}$	$4 \cdot 10^{-1}$
		Stream 2	$1 \cdot 10^{-2}$	$5 \cdot 10^{-2}$

TABLE IV
PERFORMANCE RESULTS WITH THREE TRANSMITTERS AND TWELVE RECEIVERS, RACE08

	Spectral efficiency	Data streams	Average BER	Average BLER
3IMO, QPSK	1.76 bits/s/Hz	Stream 1	$2 \cdot 10^{-2}$	$1 \cdot 10^{-1}$
		Stream 2	0	0
		Stream 3	$5 \cdot 10^{-4}$	$2 \cdot 10^{-3}$
3IMO, 8-QAM	2.64 bits/s/Hz	Stream 1	$1 \cdot 10^{-2}$	$5 \cdot 10^{-2}$
		Stream 2	$1 \cdot 10^{-3}$	$6 \cdot 10^{-3}$
		Stream 3	$8 \cdot 10^{-4}$	$3 \cdot 10^{-3}$
3IMO, 16-QAM	3.52 bits/s/Hz	Stream 1	$4 \cdot 10^{-2}$	$1.6 \cdot 10^{-1}$
		Stream 2	$1 \cdot 10^{-2}$	$4 \cdot 10^{-2}$
		Stream 3	$2 \cdot 10^{-2}$	$8 \cdot 10^{-2}$

TABLE V
PERFORMANCE RESULTS WITH FOUR TRANSMITTERS AND TWELVE RECEIVERS, RACE08

	Spectral efficiency	Data streams	Average BER	Average BLER
4IMO, QPSK	2.35 bits/s/Hz	Stream 1	$8 \cdot 10^{-2}$	$7 \cdot 10^{-2}$
		Stream 2	$2 \cdot 10^{-3}$	$4 \cdot 10^{-2}$
		Stream 3	$3 \cdot 10^{-3}$	$3 \cdot 10^{-2}$
		Stream 4	$3 \cdot 10^{-3}$	$3 \cdot 10^{-2}$
4IMO, 8-QAM	3.52 bits/s/Hz	Stream 1	$4 \cdot 10^{-1}$	$2 \cdot 10^{-1}$
		Stream 2	$7 \cdot 10^{-3}$	$1 \cdot 10^{-1}$
		Stream 3	$1 \cdot 10^{-2}$	$8 \cdot 10^{-2}$
		Stream 4	$8 \cdot 10^{-3}$	$8 \cdot 10^{-2}$

VI. PERFORMANCE RESULTS: VHF08

This experiment was conducted in the Buzzards Bay, MA, April 2008. The water depth was 12 meters. Two transmitters were about 6 meters below a surface buoy. The receiving array was about 6 meters below a boat. The array was 1 meter in aperture with 6 hydrophones. The transmission distance was 450 meters with a very high frequency (VHF) signal used. We scale the basic design of the $K = 1024$ case for the AUV07 experiment to two different bandwidths: $B = 31.25$ kHz and $B = 62.5$ kHz, following the design rules outlined in [23]. The parameters used are listed in Table VI.

TABLE VI
THE SYSTEM PARAMETERS FOR THE VHF08 EXPERIMENT

Sampling rate	$f_s = 500$ kHz
Center frequency	$f_c = 110$ kHz
OFDM block duration	$T = 65.5$ ms
Guard interval	$T_g = 20$ ms
Subcarrier spacing	$\Delta f = 15.2588$ Hz
Signal bandwidth	$B = 31.25$ kHz $B = 62.5$ kHz
Number of subcarriers	$K = 2048$
Number of data carriers	$K_d = 1344$
Number of pilot carriers	$K_p = 512$
Number of null subcarriers	$K_n = 198$
	$K_n = 396$

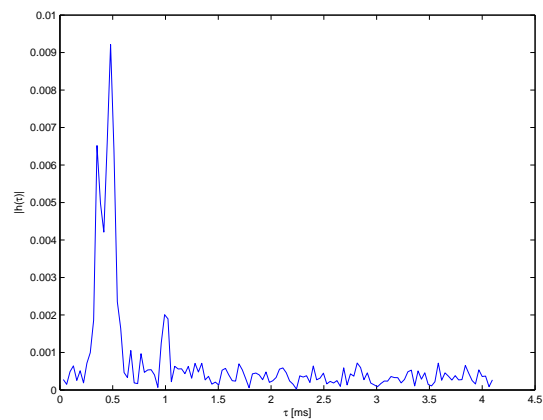


Fig. 20. Estimated channel for one OFDM block on one receiver, VHF08.

The estimated channel for one OFDM block is shown in Fig. 20. The delay spread is about 4 ms.

B. BER results

The BER results for different settings are listed in Table VII. Two transmitters and six receivers were used. The results

TABLE VII
PERFORMANCE RESULTS FOR THE VHF08 EXPERIMENT. TWO TRANSMITTERS, RATE 1/2 CODING.

	Spectral efficiency	Data rate	Data Streams	Uncoded BER	Coded BER
$B = 31.25\text{kHz}$, QPSK	1.0055 bits/s/Hz	31.4214 kb/s	Stream 1 Stream 2	0.0025 0	0 0
$B = 31.25\text{kHz}$, 8-QAM	1.5082 bits/s/Hz	47.1320 kb/s	Stream 1 Stream 2	0.0378 0.0049	0 0
$B = 31.25\text{kHz}$, 16-QAM	2.0010 bits/s/Hz	62.8438 kb/s	Stream 1 Stream 2	0.0868 0.0319	0 0
$B = 62.5\text{kHz}$, QPSK	1.0055 bits/s/Hz	62.8427 kb/s	Stream 1 Stream 2	0.0512 0.0193	0 0
$B = 62.5\text{kHz}$, 8-QAM	1.5082 bits/s/Hz	94.2640 kb/s	Stream 1 Stream 2	0.1102 0.0488	0 0
$B = 62.5\text{kHz}$, 16-QAM	2.0110 bits/s/Hz	125.6875 kb/s	Stream 1 Stream 2	0.1938 0.1290	0 0

are based on the iterative receiver with rate 1/2 nonbinary LDPC coding. There were 36, 24, and 18 OFDM blocks for the cases of QPSK, 8-QAM, and 16-QAM, respectively, when $B = 31.25\text{ kHz}$. There were 18, 12, and 9 OFDM blocks for the cases of QPSK, 8-QAM, and 16-QAM, respectively, when $B = 62.5\text{ kHz}$. Therefore, the BER values in Table VII are averaged over $1344 \times 36 = 48,384$ information bits for each parallel data stream at each setting. Error-free performance is achieved in this data set after no more than two rounds of iterative demodulation and decoding.

VII. CONCLUSIONS

In this paper, a MIMO-OFDM system with spatial multiplexing was presented. The receiver works on a block-by-block basis where null and pilot subcarriers are used for Doppler and channel estimation, respectively, and an iterative structure is used for MIMO detection and decoding. We reported on the performance results based on data processing from three different experiments, showing very high spectral efficiency via parallel data multiplexing with high order constellations. These example results suggest that MIMO-OFDM is an appealing choice for high data rate underwater acoustic communications.

Further investigations on MIMO underwater acoustic communications, both single- and multi-carrier approaches, are warranted, especially on the capacity limits in underwater channels, advanced receiver designs, and experimental results in more challenging channel conditions with large Doppler spread.

APPENDIX: MMSE EQUALIZATION WITH A PRIORI INFORMATION [17]

For convenience, we list here the MMSE equalization algorithm with *a priori* information from [17].

We omit the index k and the subscript in (6) to work on a generic model $\mathbf{z} = \mathbf{As} + \boldsymbol{\xi}$, where $\boldsymbol{\xi}$ has a covariance matrix $\sigma_w^2 \mathbf{I}_N$. The *a priori* information of s_n , $n = 1, 2, \dots, N$, is given in the forms of the mean $\bar{s}_n \triangleq E(s_n)$ and the variance $v_n \triangleq \text{Cov}(s_n, s_n)$. Let \mathbf{a}_n denote the n -th column of matrix

\mathbf{A} , and use \bar{s}_n and v_n to define:

$$\bar{\mathbf{s}} \triangleq E(\mathbf{s}) = [\bar{s}_1, \bar{s}_2, \dots, \bar{s}_N]^T, \quad (9)$$

$$\bar{\mathbf{z}} \triangleq E(\mathbf{z}) = \mathbf{A}\bar{\mathbf{s}} = \mathbf{A}\bar{\mathbf{s}}, \quad (10)$$

$$\mathbf{V} \triangleq \text{Cov}(\mathbf{s}, \mathbf{s}) = \text{diag}[v_1, v_2, \dots, v_N], \quad (11)$$

$$\boldsymbol{\Sigma} \triangleq \text{Cov}(\mathbf{z}, \mathbf{z}) = \sigma_w^2 \mathbf{I}_N + \mathbf{AV}\mathbf{A}^H, \quad (12)$$

$$\mathbf{f}_n \triangleq \boldsymbol{\Sigma}^{-1} \mathbf{a}_n, \quad (13)$$

$$K_n \triangleq (1 + (1 - v_n)\mathbf{f}_n^H \mathbf{a}_n)^{-1}. \quad (14)$$

The estimate \hat{s}_n is then computed as

$$\hat{s}_n = K_n \cdot \mathbf{f}_n^H (\mathbf{z} - \bar{\mathbf{z}} + \bar{s}_n \mathbf{a}_n). \quad (15)$$

In this computation, \hat{s}_n is independent from the *a priori* information about s_n , but dependent on the *a priori* information about all $s_{n'}$ where $n' \neq n$ [17].

Assuming that \hat{s}_n is Gaussian distributed with mean

$$\mu_n = K_n \cdot s_n \cdot \mathbf{f}_n^H \mathbf{a}_n \quad (16)$$

and variance

$$\sigma_n^2 = K_n^2 \cdot (\mathbf{f}_n^H \mathbf{a}_n - v_n \mathbf{f}_n^H \mathbf{a}_n \mathbf{a}_n^H \mathbf{f}_n), \quad (17)$$

the probabilities $p(\hat{s}_n | s_n = \alpha_i)$, $i = 1, 2, \dots, M$, can be computed from Gaussian probability density function [17]. These probabilities are passed to the nonbinary LDPC decoder.

ACKNOWLEDGEMENT

We are grateful to Dr. James Preisig and his team for conducting the RACE08 experiment.

REFERENCES

- [1] B. Li, S. Zhou, M. Stojanovic, L. Freitag, J. Huang, and P. Willett, "MIMO-OFDM over an underwater acoustic channel," in *Proc. of MTS/IEEE OCEANS conference*, Vancouver, BC, Canada, Sept. 29 - Oct. 4, 2007.
- [2] B. Li, J. Huang, S. Zhou, K. Ball, M. Stojanovic, L. Freitag, and P. Willett, "Further results on high-rate MIMO-OFDM underwater acoustic communications," in *Proc. of MTS/IEEE OCEANS conference*, Quebec City, Canada, Sept. 2008.
- [3] E. Telatar, "Capacity of multi-antenna Gaussian channels," *Technical Memorandum, AT&T Bell Laboratories*, Oct. 1995.
- [4] G. J. Foschini and M. J. Gans, "On limits of wireless communication in a fading environment when using multiple antennas," *Wireless Personal Communications*, vol. 6, no. 3, pp. 311–335, Mar. 1998.
- [5] D. B. Kilfoyle, J. C. Preisig, and A. B. Bagherer, "Spatial modulation experiments in the underwater acoustic channel," *IEEE Journal of Oceanic Engineering*, vol. 30, no. 2, pp. 406–415, Apr. 2005.

- [6] S. Roy, T. M. Duman, V. McDonald, and J. G. Proakis, "High rate communication for underwater acoustic channels using multiple transmitters and space-time coding: Receiver structures and experimental results," *IEEE Journal of Oceanic Engineering*, vol. 32, no. 3, pp. 663–688, July 2007.
- [7] H. C. Song, W. S. Hodgkiss, W. A. Kuperman, T. Akal, and M. Stevenson, "Multiuser communications using passive time reversal," *IEEE Journal of Oceanic Engineering*, vol. 32, no. 4, pp. 915–926, October 2007.
- [8] A. Song, M. Badiey, and V. K. McDonald, "Multi-channel combining and equalization for underwater acoustic MIMO channels," in *Proc. of MTS/IEEE OCEANS conference*, Quebec City, Canada, Sept. 15–18, 2008.
- [9] J. Tao, Y. R. Zheng, C. Xiao, T. C. Yang, and W.-B. Yang, "Time-domain receiver design for MIMO underwater acoustic communications," in *Proc. of MTS/IEEE OCEANS conference*, Quebec City, Canada, Sept. 15–18, 2008.
- [10] J. Zhang, Y. R. Zheng, and C. Xiao, "Frequency-domain equalization for single carrier MIMO underwater acoustic communications," in *Proc. of MTS/IEEE OCEANS conference*, Quebec City, Canada, Sept. 15–18, 2008.
- [11] F. Qu and L. Yang, "Basis expansion model for underwater acoustic channels?" in *Proc. of MTS/IEEE OCEANS conference*, Quebec City, Canada, Sept. 15–18, 2008.
- [12] P. Carrascosa and M. Stojanovic, "Adaptive MIMO detection of OFDM signals in an underwater acoustic channel," in *Proc. of MTS/IEEE OCEANS conference*, Quebec City, Canada, Sept. 15–18, 2008.
- [13] Y. Emre, V. Kandasamy, T. M. Duman, P. Hursky, and S. Roy, "Multi-input multi-output OFDM for shallow-water UWA communications," in *Acoustics'08 Conference*, Paris, France, July 2008.
- [14] B. Li, S. Zhou, M. Stojanovic, L. Freitag, and P. Willett, "Multicarrier communication over underwater acoustic channels with nonuniform Doppler shifts," *IEEE Journal of Oceanic Engineering*, vol. 33, no. 2, pp. 198–209, Apr. 2008.
- [15] M. Stojanovic, "Low complexity OFDM detector for underwater channels," in *Proc. of MTS/IEEE OCEANS conference*, Boston, MA, Sept. 18–21, 2006.
- [16] ———, "OFDM for underwater acoustic communications: Adaptive synchronization and sparse channel estimation," in *Proc. of Intl. Conf. on ASSP*, Las Vegas, NV, Mar. 30 – Apr. 4, 2008.
- [17] M. Tuchler, A. C. Singer, and R. Koetter, "Minimum mean squared error equalization using a priori information," *IEEE Transactions on Signal Processing*, vol. 50, no. 3, pp. 673–683, Mar. 2002.
- [18] J. Huang, S. Zhou, and P. Willett, "Nonbinary LDPC coding for multicarrier underwater acoustic communication," *IEEE J. Select. Areas Commun.*, vol. 26, no. 9, pp. 1684–1696, Dec. 2008.
- [19] T. Kang and R. A. Iltis, "Iterative carrier frequency offset and channel estimation for underwater acoustic OFDM systems," *IEEE J. Select. Areas Commun.*, vol. 26, no. 9, pp. 1650–1661, Dec. 2008.
- [20] G. B. Giannakis, Z. Liu, X. Ma, and S. Zhou, *Space Time Coding for Broadband Wireless Communications*. John Wiley & Sons, Inc., Dec. 2006.
- [21] C. R. Berger, S. Zhou, J. C. Preisig, and P. Willett, "Sparse channel estimation for multicarrier underwater acoustic communication: From subspace methods to compressed sensing," in *Proc. of MTS/IEEE OCEANS conference*, Bremen, Germany, May 11–14, 2009.
- [22] J. G. Proakis, *Digital Communications*, McGraw-Hill, 4th edition, 2001.
- [23] B. Li, S. Zhou, J. Huang, and P. Willett, "Scalable OFDM design for underwater acoustic communications," in *Proc. of Intl. Conf. on ASSP*, Las Vegas, NV, Mar. 30 – Apr. 4, 2008.



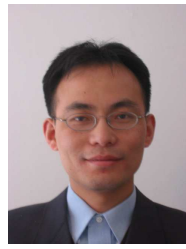
Baosheng Li (S'05) received the B.S. and the M.S. degrees in the electronic and communications engineering from the Harbin Institute of Technology, Harbin, China, in 2002 and 2004, respectively. He received his Ph.D. degree in electrical engineering from the University of Connecticut, Storrs, in 2009. He is currently a postdoctoral research fellow at Northeastern University, Boston, MA.

His research interests lie in the areas of communications and signal processing, currently focusing on multi-transceiver and multi-carrier modulation algorithms for underwater acoustic communications.



Jie Huang received the B.S. degree in 2001 and the Ph. D. degree in 2006, from the University of Science and Technology of China (USTC), Hefei, both in electrical engineering and information science. He was a post-doctoral researcher with the Department of Electrical and Computer Engineering at the University of Connecticut (UCONN), Storrs, from July 2007 to June 2009, and is now a research assistant professor at the University of Connecticut (UCONN), Storrs.

His general research interests lie in the areas of communications and signal processing, specifically error control coding theory and coded modulation. His recent focus is on signal processing, channel coding and network coding for underwater acoustic communications and networks.



Shengli Zhou (M'03) received the B.S. degree in 1995 and the M.Sc. degree in 1998, from the University of Science and Technology of China (USTC), Hefei, both in electrical engineering and information science. He received his Ph.D. degree in electrical engineering from the University of Minnesota (UMN), Minneapolis, in 2002. He has been an assistant professor with the Department of Electrical and Computer Engineering at the University of Connecticut (UCONN), Storrs, 2003–2009, and now is an associate professor. He holds a United Technologies Corporation (UTC) Professorship in Engineering Innovation, 2008–2011.

His general research interests lie in the areas of wireless communications and signal processing. His recent focus is on underwater acoustic communications and networking. Dr. Zhou has served as an associate editor for IEEE Transactions on Wireless Communications from Feb. 2005 to Jan. 2007, and is now an associate editor for IEEE Transactions on Signal Processing. He received the 2007 ONR Young Investigator award and the 2007 Presidential Early Career Award for Scientists and Engineers (PECASE).



Keenan Ball holds a BS from Wentworth Institute of Technology in Electromechanical Engineering and an MS from the University of Massachusetts Dartmouth in Electrical Engineering which he received in 2000 and 2002 respectively. He is currently a Research Engineer at the Woods Hole Oceanographic Institution where he has worked on projects related to underwater acoustics. The programs that he works on focus on underwater acoustic communication and navigation for UUVs, moored systems, and the associated hardware designs for these applications.



Milica Stojanovic (M'93) graduated from the University of Belgrade, Serbia, in 1988, and received the M.S. and Ph.D. degrees in electrical engineering from Northeastern University, Boston, MA, in 1991 and 1993. After a number of years with the Massachusetts Institute of Technology, where she was a Principal Scientist, she joined the faculty of Electrical and Computer Engineering Department at Northeastern University in 2008. She is also a Guest Investigator at the Woods Hole Oceanographic Institution, and a Visiting Scientist at MIT.

Her research interests include digital communications theory, statistical signal processing and wireless networks, and their applications to mobile radio and underwater acoustic communication systems. Milica is an Associate Editor for the IEEE Journal of Oceanic Engineering and the IEEE Transactions on Signal processing.



Lee Freitag (M'88) holds BS and MS degrees in Electrical Engineering from the University of Alaska, Fairbanks, which he received in 1986 and 1987 respectively. He is currently a Senior Engineer at the Woods Hole Oceanographic Institution where he has worked on projects related to underwater acoustics for 15 years.

His research programs focus on underwater acoustic communication and navigation with a strong focus on UUVs, sensors and submarine systems. He is a member of IEEE and MTS.



Peter Willett (F'03) received his BASc (Engineering Science) from the University of Toronto in 1982, and his PhD degree from Princeton University in 1986. He has been a faculty member at the University of Connecticut ever since, and since 1998 has been a Professor. His primary areas of research have been statistical signal processing, detection, machine learning, data fusion and tracking. He has interests in and has published in the areas of change/abnormality detection, optical pattern recognition, communications and industrial/security condition monitoring.

He is editor-in-chief for IEEE Transactions on Aerospace and Electronic Systems, and until recently was associate editor for three active journals: IEEE Transactions on Aerospace and Electronic Systems (for Data Fusion and Target Tracking) and IEEE Transactions on Systems, Man, and Cybernetics, parts A and B. He is also associate editor for the IEEE AES Magazine, editor of the AES Magazine periodic Tutorial issues, associate editor for ISIF electronic Journal of Advances in Information Fusion, and is a member of the editorial board of IEEE Signal Processing Magazine. He has been a member of the IEEE AESS Board of Governors since 2003. He was General Co-Chair (with Stefano Coraluppi) for the 2006 ISIF/IEEE Fusion Conference in Florence, Italy, Program Co-Chair (with Eugene Santos) for the 2003 IEEE Conference on Systems, Man, and Cybernetics in Washington DC, and Program Co-Chair (with Pramod Varshney) for the 1999 Fusion Conference in Sunnyvale.